Controlling single and few-layer graphene crystals growth in a solid carbon source based chemical vapor deposition

Remi Papon, Golap Kalita, Subash Sharma, Sachin M. Shinde, Riteshkumar Vishwakarma, and Masaki Tanemura

Articles you may be interested in

Local solid phase growth of few-layer graphene on silicon carbide from nickel silicide supersaturated with carbon
J. Appl. Phys. **113**, 114309 (2013); 10.1063/1.4795501

Controllable chemical vapor deposition of large area uniform nanocrystalline graphene directly on silicon dioxide
J. Appl. Phys. **111**, 044103 (2012); 10.1063/1.3686135

Quantum Hall effect on centimeter scale chemical vapor deposited graphene films
Appl. Phys. Lett. **99**, 232110 (2011); 10.1063/1.3663972

Direct growth of few-layer graphene on 6H-SiC and 3C-SiC/Si via propane chemical vapor deposition
Appl. Phys. Lett. **97**, 171909 (2010); 10.1063/1.3503972

Microcrystalline, nanocrystalline, and ultrananocrystalline diamond chemical vapor deposition: Experiment and modeling of the factors controlling growth rate, nucleation, and crystal size
J. Appl. Phys. **101**, 053115 (2007); 10.1063/1.2696363

Controlling single and few-layer graphene crystals growth in a solid carbon source based chemical vapor deposition

Remi Papon,[1] Golap Kalita,[1,2,a)] Subash Sharma,[1] Sachin M. Shinde,[1] Riteshkumar Vishwakarma,[1] and Masaki Tanemura[1]

[1]*Department of Frontier Materials, Nagoya Institute of Technology, Gokiso-cho, Showa-ku, Nagoya 466-8555, Japan*
[2]*Center for Fostering Young and Innovative Researchers, Nagoya Institute of Technology, Gokiso-cho, Showa-ku, Nagoya, 466-8555, Japan*

Here, we reveal the growth process of single and few-layer graphene crystals in the solid carbon source based chemical vapor deposition (CVD) technique. Nucleation and growth of graphene crystals on a polycrystalline Cu foil are significantly affected by the injection of carbon atoms with pyrolysis rate of the carbon source. We observe micron length ribbons like growth front as well as saturated growth edges of graphene crystals depending on growth conditions. Controlling the pyrolysis rate of carbon source, monolayer and few-layer crystals and corresponding continuous films are obtained. In a controlled process, we observed growth of large monolayer graphene crystals, which interconnect and merge together to form a continuous film. On the other hand, adlayer growth is observed with an increased pyrolysis rate, resulting few-layer graphene crystal structure and merged continuous film. The understanding of monolayer and few-layer crystals growth in the developed CVD process can be significant to grow graphene with controlled layer numbers. © 2014 AIP Publishing LLC. [http://dx.doi.org/10.1063/1.4896845]

Considering the extraordinary properties of graphene for various applications, synthesis of high quality graphene in large-area is gaining remarkable attention.[1–5] In the last few years, significant efforts have been made to synthesize large-area graphene by *atmospheric* or *low pressure* CVD techniques using methane as primary carbon source gas.[5–7] Continuous single layer graphene has been synthesized on Cu foil by low-pressure CVD process. At the same time, recent studies show that significant high quality graphene can be synthesized by a simple atmospheric-pressure CVD.[8,9] It has been observed that continuous graphene films synthesized on polycrystalline metal foils by a CVD process are constituted with interconnections of several domains.[9–12] Hence, the electrical, optical, and mechanical properties of a CVD graphene film are significantly influenced by the domain quality, size, and structures.[13,14] Thus, significant importance has been given for growth of large domains and single crystal structure to overcome the effects of grain boundaries. Synthesis of large size graphene crystals has been reported on Cu foil using both low and atmospheric-pressure CVD techniques.[14–19]

Similarly, significant interest has been given to bilayer graphene structure considering its interesting electronic properties unlike monolayer graphene.[20,21] Most recently, synthesis of AB-stacked or twisted bilayer single crystal graphene by a CVD process has been demonstrated.[22] The quality of individual graphene crystals synthesized by CVD approaches is significantly influenced by the experimental conditions and source materials. Recently, solid precursors have also been used for high quality graphene synthesis in a simplified CVD approach.[8,23] We have demonstrated

synthesis of graphene crystals using camphor and waste plastic as solid carbon source in an ambient pressure (AP) CVD process, this facilitates us to convert waste into a significantly value added form of material.[8] However, the injection rate of carbon compounds from the solid source can considerably influence graphene growth and requires much better control to obtain high quality graphene. Subsequently, the understanding of graphene growth process in a solid source based CVD process can be significant in controlling growth of single and few-layer graphene. In this prospect, we have investigated the growth of single and few-layer graphene crystals on Cu foil using waste plastic as a carbon source.

In this study, Cu foil (Nilaco Corp.) with a thickness of $20\,\mu m$ and purity of 99.98% was used as a substrate for graphene synthesis. Solid waste plastic used for material packaging is used as carbon source. Cu substrate was annealed for 30 min in 100 standard cubic centimeters per minute (sccm) of H_2 at $1020\,^\circ C$, prior to introduction of the carbon source. 3 mg of waste plastic was placed in the quartz tube and slowly pyrolyzed increasing the temperature up to $480\,^\circ C$. The pyrolyzed carbon source was injected in the graphene growth zone with a gas mixture of Ar and H_2. The growth of graphene crystals was investigated with variation of heating rate of solid waste plastic (1–$3\,^\circ C/min$). Morphological and structural analyses of synthesized graphene crystals were carried out by optical microscope, scanning electron microscope (SEM), and Raman spectroscopy. Optical microscope studies were carried out by using VHX-5000. SEM studies of graphene crystals were carried out with Hitachi S-4300 at an operating voltage of $20\,kV$. Raman spectra were obtained using NRS 3300 laser Raman spectrometer with laser excitation energy of 532.08 nm from a green laser.

The waste plastic used for graphene synthesis is generally constituted with polyethylene and polystyrene

a)Author to whom correspondence should be addressed. Electronic mail: kalita.golap@nitech.ac.jp. Tel./Fax: +81-52-735-5216.
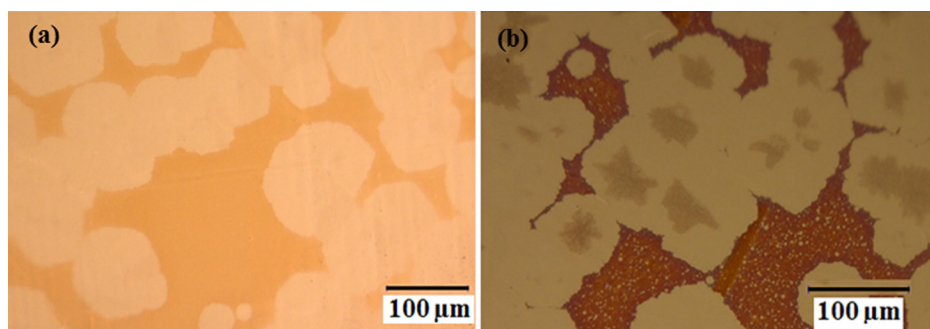
FIG. 1. Optical microscope images of round-shaped graphene crystals synthesized on Cu foil with (a) lower (1.5 °C/min.) and (b) higher (>1.5 °C/min) pyrolysis rate of waste plastic pyrolysis.

components. Synthesis of graphene crystals and continuous films was investigated by pyrolysis of source materials and injection rate. Figure 1(a) shows optical microscope image of round-shaped graphene crystals synthesized on Cu foil with a waste plastic pyrolysis rate of 1.5 °C/min. Synthesized graphene crystals are uniformly single layer structure without much defects. Similarly, Figure 1(b) shows optical microscope image of graphene crystals with a higher (>1.5 °C/min) pyrolysis rate of source materials. We observed micron size dark areas in the center part of most crystals. The color contrast within the crystal signifies variation in number of layers. Graphene crystals with size of 10–100 μm were obtained, where the number of layers in the center part varies from bi-layer to few layer as confirmed by Raman studies with crystals size of 10–50 μm. This shows that the pyrolysis rate of waste plastic, and thereby the injection of carbon atoms is playing a critical role in the crystal growth process. As follows, we discuss the crystal growth process of single and few-layer graphene to achieve controlled growth.

The injection of carbon atoms and growth conditions in the CVD process also affect structure of individual crystals obtained on Cu foil. Figures 2(a) and 2(b) show optical microscope images of graphene crystals with unsaturated growth edges, when the carbon source supply was stopped abruptly. We observe micron length ribbons at crystal edges, which are the growth front of the crystal. The length of these

micro-ribbons is in the range of 1.5–6 μm, where aspect ratio is higher for some ribbons. This suggests that continuous supply of carbon atoms with pyrolysis of waste plastic is necessary to achieve growth of a larger crystal. Figure 2(c) shows saturated growth edge of a graphene crystal without any presence of microribbon growth front. In this experiment, we did not stop the precursor injection in the growth zone and graphene growth was performed by normal process. The observation of graphene growth with or without microribbon signifies the importance of CVD parameters.

Figure 3 shows SEM images of individual graphene crystals and their merged structure to form a continuous film. The growth of single layer crystals and merged structure is obtained with a pyrolysis rate of 1.5 °C/min. Hexagonal graphene crystals are the ideal building blocks of large-area continuous films. We observed growth of ∼100 μm large graphene crystals on Cu foil using waste plastic as carbon source. The individual graphene crystals were interconnected each other with increased growth duration as shown in Figures 3(b) and 3(c). Individual graphene crystals grow further and thereby merge together to form a continuous film. Figure 3(d) shows formation of a continuous graphene film, where white spots are the remaining void of incomplete growth. The observation of crystal growth and merged continuous monolayer graphene film with a controlled pyrolysis rate of waste plastic can be significant for large-area synthesis.

Individual and merged graphene crystals are further analyzed with optical microscope and Raman studies. Figure 4(a) shows an optical microscope image of graphene grown on Cu foil with the pyrolysis rate of 1.5 °C/min as discussed above. It has been observed that graphene growth is uniform at this pyrolysis rate of the carbon source. We do not observe structural or morphological defects in single layer crystal, which is the case with a higher pyrolysis rate. Graphene crystals were analyzed by Raman spectroscopy at various points to confirm uniformity of crystal structure. Figure 4(b) shows Raman spectra at four different points of one crystal. Raman spectra show a very small defect induced D peak, confirming high quality of graphene crystal. Graphitic G and second order 2D Raman peaks are observed at 1586 and 2702 cm^{-1}, respectively. The higher intensity of 2D peak than that of G peak signifies growth of single layer graphene. Full width at half maximum (FWHM) of G and 2D peaks are found to be 19 and 44.2 cm^{-1}, respectively, consistent with previous results. Raman, optical microscope, and SEM studies confirmed growth of single layer and their merged graphene structure.

Figure 5 shows synthesized graphene crystals with a much higher pyrolysis rate (3 °C/min) for the waste plastic.
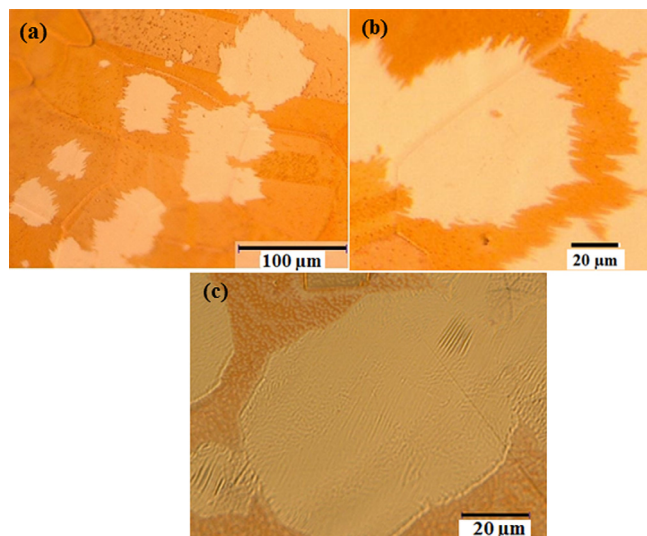

FIG. 2. Optical microscope images of graphene crystals with (a) micron length ribbons at the crystals edges, (b) saturated growth edge of a graphene crystal.
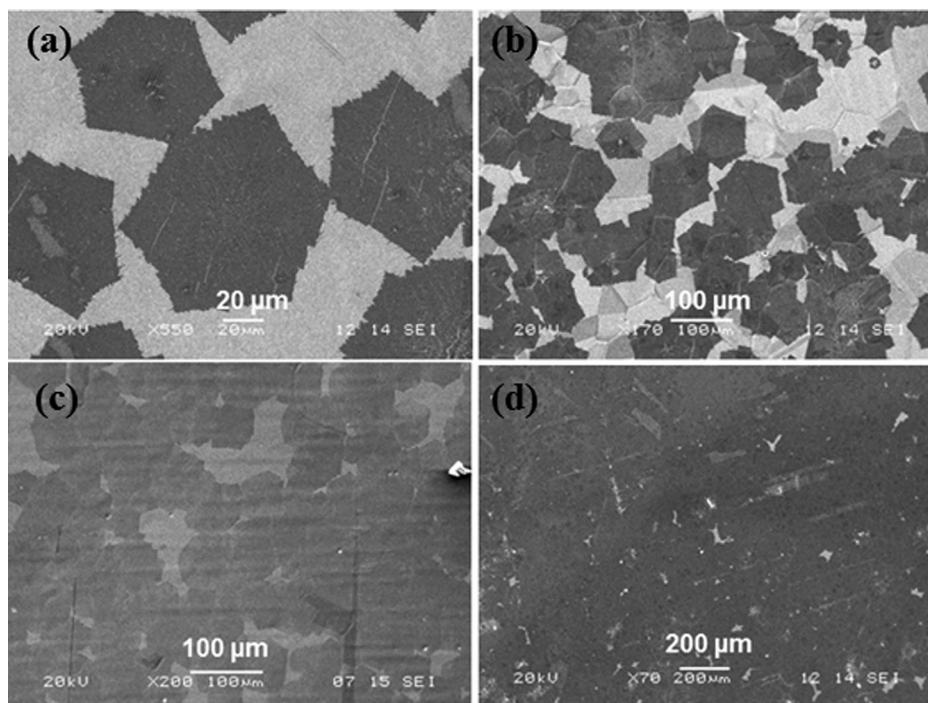
FIG. 3. SEM images of (a) individual hexagonal graphene crystal (b), (c) interconnected graphene crystals, and (c) merged structure to form a continuous film with a pyrolysis temperature increase rate of 1.5 °C/min of the waste plastic.

Increasing the pyrolysis rate, significant amount of polymeric compounds was generated and injected to the growth zone. High amount of carbon radicals was formed with decomposition of polymeric compounds, which significantly influences graphene growth. Figure 5(a) shows SEM image of individual graphene crystals with more than single layer at the center, which is a sharp contrast to the morphology obtained at a lower pyrolysis rate. As shown in optical microscope studies, we observed graphene crystals with size of 10–100 μm, where the number of layers in the center part varies from bi-layer to few layer with crystals size of 10–30 μm. The individual graphene crystals grow further and merged together as shown in Figures 5(b) and 5(c). Merging of these crystals is also similar to that of the previous case of a single layer graphene. Figure 5(c) presents highly dense merged structure of crystals, where dark areas can be directly identified as few-layer graphene. Figure 5(d) shows a continuous graphene film with interconnected crystals of single and few-layer graphene. Thus, uneven growth of single and few-layer graphene in the continuous film is observed with a higher pyrolysis rate.

Figure 6(a) presents higher resolution SEM image of graphene crystals with few-layer morphology at the center. Raman studies were performed to confirm the structure of synthesized graphene crystals. Figure 6(b) shows Raman spectra at two different positions (1 and 2) of a crystal. The two spectra at positions 1 and 2 are distinctly different from each other. Graphitic G and second order 2D Raman peaks are observed around 1590 and 2705 cm^{-1}, respectively. The intensity ratio of 2D to G peak at position 1 is much lower than that of position 2. The FWHM of 2D and G peaks for graphene in the center part of a crystal (position 1) is found to be 17.9 and 45.1 cm^{-1}, respectively. Again, for the Raman spectra in position 2, it is found to be 16.6 and 37.9 cm^{-1}, respectively. The peak intensity ratio and FWHM results clearly indicate growth of few-layer graphene at the center position. Figure 6(c) shows a schematic diagram of graphene growth process on Cu foil in the developed CVD process. We obtained growth of single layer graphene crystals and their merged structure to form a continuous film with a controlled and low pyrolysis rate. On the other hand, increasing the pyrolysis rate, we observed growth of bi-layer and few-layer graphene crystals with higher carbon atoms injection. The growth of adlayer within the individual graphene crystals and their merged structure produces few-layer continuous film. Growth of adlayer can occurs with diffusion of carbon from the crystal edge or with primarily diffused carbon atoms in the Cu surface. Previously, in a methane CVD
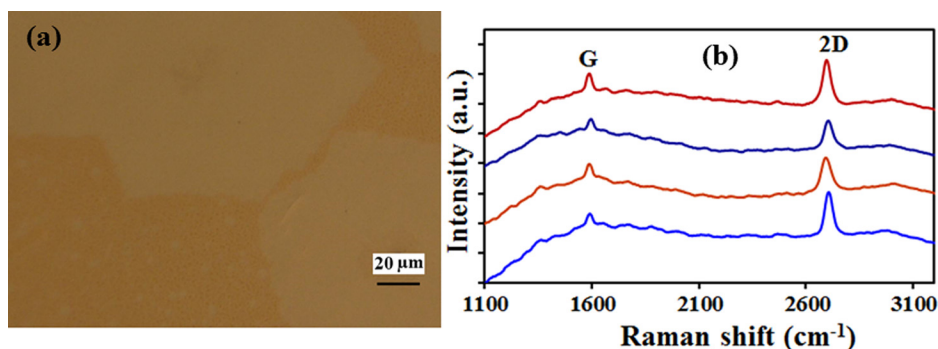

FIG. 4. (a) Optical microscope image of single layer graphene crystals on Cu foil. (b) Raman spectra taken at four different points of the graphene.
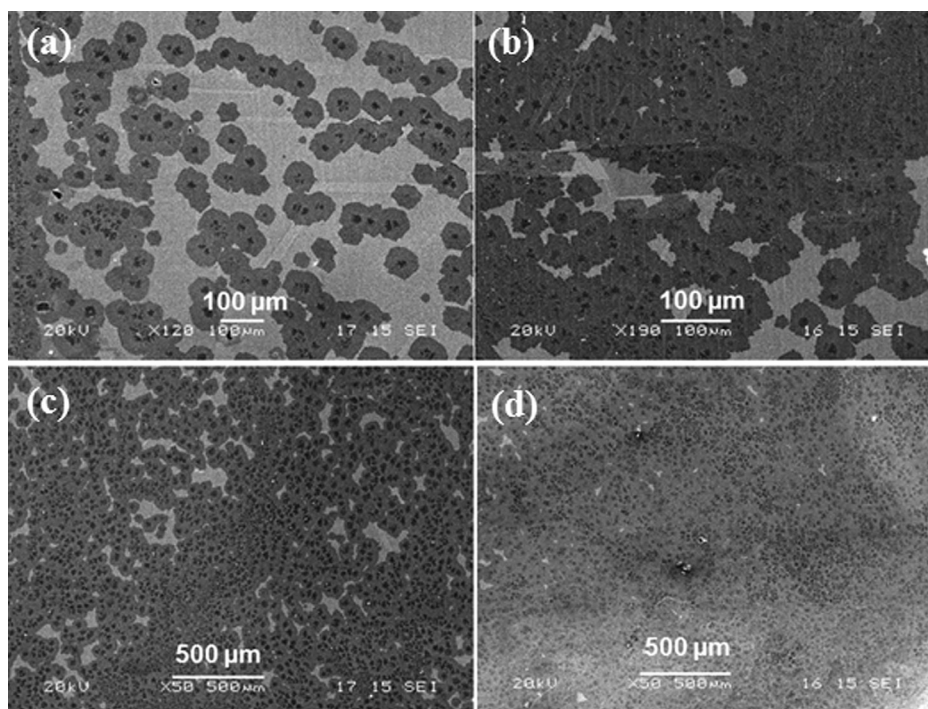
FIG. 5. SEM image of (a) individual (b), (c) interconnected and (d) merged graphene crystal structure with a much higher pyrolysis temperature increase rate (3 °C/min) of the solid carbon source.

process, growth of few-layer graphene crystals has been observed with a high methane flow rate.[24] Vlassiouk *et al.* found that single layer dendrite shape graphene crystals were grown on Cu surface at a low H_2 pressure, while at a higher H_2 pressure regular hexagonal shape of bi-layer and few-layer graphene were obtanied.[9] Similarly, Zhang *et al.* reported graphene edge termination with H atoms and detaching from the Cu surface at a higher H_2 pressure, which enables diffusion of C species underneath of individual crystal for adlayer growth.[25] In respect to previous studies, we found that not only the H_2 pressure but also the amount of injected carbon compounds play a critical role in the growth of graphene crystal. Changing the injection rate of carbon precursor at the same Ar:H_2 pressure ratio, single or few-layer graphene crystals were obtained. This is may be due to the primarily absorbed carbon atoms in the Cu surface, which contribute to the growth of the adlayer to form bilayer and few-layer graphene crystals.
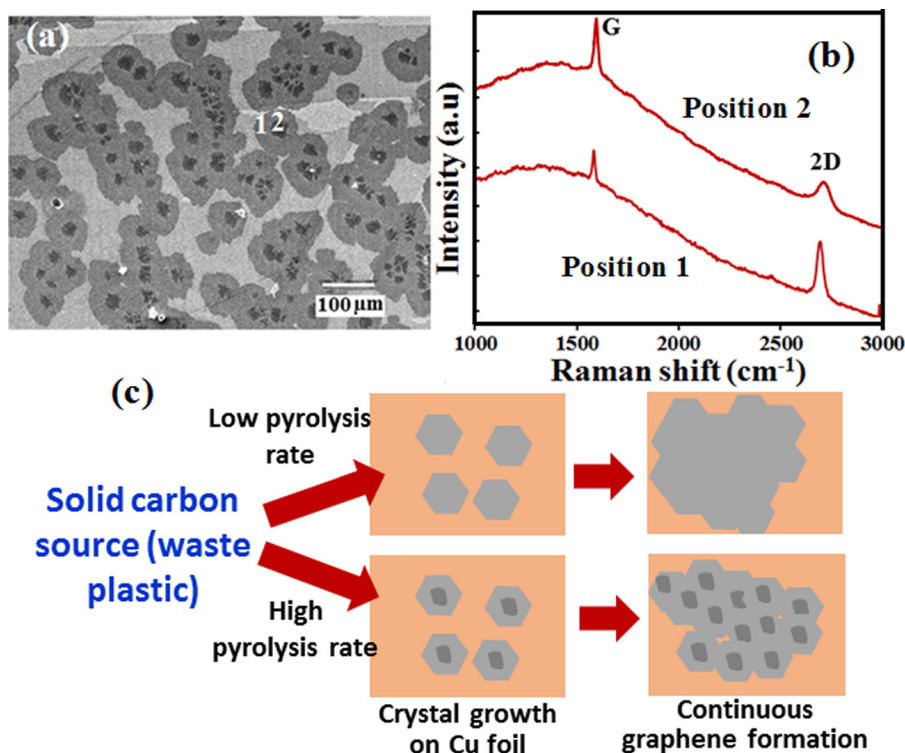

FIG. 6. (a) SEM image of individual graphene crystals with few-layer morphology. (b) Raman studies of a graphene crystal at two different points (position 1 and 2). (c) Schematic diagram of the graphene growth process on Cu foil in the developed CVD process.

In summary, we have revealed the growth process of single and few-layer graphene crystals in the solid carbon source based CVD technique. Nucleation and growth of graphene crystals on a Cu foil were significantly affected by the increase of pyrolysis rate (1–3 °C/min) of the solid waste plastic. We observed micron length ribbons like growth front as well as saturated growth edges of graphene crystals with or without abrupt interruption of the CVD growth process, respectively. Controlling pyrolysis of the carbon source (1.5 °C/min), growth of large monolayer graphene crystals and corresponding continuous graphene films were achieved. On the other hand, bi-layer and few-layer graphene crystals structure were obtained increasing the pyrolysis rate (3 °C/min). The understanding of monolayer and few-layer crystals growth in the developed CVD process can be significant to grow graphene with controlled layer numbers.

[1] K. S. Novoselov, A. K. Geim, S. V. Morozov, D. Jiang, M. I. Katsnelson, I. V. Grigorieva, S. V. Dubonos, and A. A. Firsov, Nature **438**, 197 (2005).

[2] Y. Zhang, Y. W. Tan, H. L. Stormer, and P. Kim, Nature **438**, 201 (2005).

[3] S. V. Morozov, K. S. Novoselov, M. I. Katsnelson, F. Schedin, D. C. Elias, J. A. Jaszczak, and A. K. Geim, Phys. Rev. Lett. **100**, 016602 (2008).

[4] S. Stankovich, D. A. Dikin, G. H. Dommett, K. M. Kohlhaas, E. J. Zimney, E. A. Stach, R. D. Piner, S. T. Nguyen, and R. S. Ruoff, Nature **442**, 282 (2006).

[5] S. Bae, H. K. Kim, Y. Lee, X. Xu, J. Park, Y. Zheng, J. Balakrishnan, D. Im, T. Lei, Y. Song, Y. Kim, K. Kim, B. Ozyimaz, J. Ahn, B. Hong, and S. Iijima, Nat. Nanotechnol. **5**, 574 (2010).

[6] K. S. Kim, Y. Zhao, H. Jang, S. Y. Lee, J. M. Kim, K. S. Kim, J. H. Ahn, P. Kim, J. Y. Choi, and B. H. Hong, Nature **457**, 706 (2009).

[7] X. S. Li, W. W. Cai, J. H. An, S. Kim, J. Nah, D. X. Yang, R. Piner, A. Velamakanni, I. Jung, E. Tutuc, S. K. Banerjee, L. Colombo, and R. S. Ruoff, Science **324**, 1312 (2009).

[8] S. Sharma, G. Kalita, R. Hirano, S. M. Shinde, R. Papon, H. Ohtani, and M. Tanemura, Carbon **72**, 66 (2014).

[9] I. Vlassiouk, P. Fulvio, H. Meyer, N. Lavrik, S. Dai, P. Datskos, and S. Smirnov, Carbon **54**, 58 (2013).

[10] C. Wang, W. Chen, C. Han, G. Wang, B. Tang, C. Tang, Y. Wang, W. Zou, W. Chen, X. A. Zhang, S. Qin, S. Chang, and L. Wang, Sci. Rep. **4**, 4537 (2014).

[11] C. Hwang, K. Yoo, S. J. Kim, E. K. Seo, H. Yu, and L. P. Biró, Jour. Phys. Chem. C **115**, 22369 (2011).

[12] D. Geng, B. Wu, Y. Guo, L. Huang, Y. Xue, J. Chen, G. Yu, L. Jiang, W. Hu, and Y. Liu, Proc. Natl. Acad. Sci. **109**, 7992 (2012).

[13] D. A. Abanin and L. S. Levitov, Phys. Rev. B **78**, 035416 (2008).

[14] H. Wang, G. Wang, P. Bao, S. Yang, W. Zhu, X. Xie, and W. J. Zhang, J. Am. Chem. Soc. **134**, 3627 (2012).

[15] L. Gao, W. Ren, H. Xu, L. Jin, Z. Wang, T. Ma, L. P. Ma, Z. Zhang, Q. Fu, L. M. Peng, X. Bao, and H. M. Cheng, Nat. Commun. **3**, 699 (2012).

[16] T. Wu, G. Ding, H. Shen, H. Wang, L. Sun, D. Jiang, X. Xie, and M. Jiang, Adv. Funct. Mater. **23**, 198 (2013).

[17] Z. Yan, J. Lin, Z. Peng, Z. Sun, Y. Zhu, L. Li, C. Xiang, E. L. Samuel, C. Kittrell, and J. M. Tour, ACS Nano **6**, 9110 (2012).

[18] W. Wu, L. A. Jauregui, Z. Su, Z. Liu, J. Bao, Y. P. Chen, and Q. Yu, Adv. Mater. **23**, 4898 (2011).

[19] H. Zhou, W. J. Yu, L. Liu, R. Cheng, Y. Chen, X. Huang, Y. Liu, Y. Wang, Y. Huang, and X. Duan, Nat. Commun. **4**, 2096 (2013).

[20] T. Ohta, A. Bostwick, T. Seyller, K. Horn, and E. Rotenberg, Science **313**, 951 (2006).

[21] S. Lee, K. Lee, and Z. Zhong, Nano Lett. **10**, 4702 (2010).

[22] C. C. Lu, Y. C. Lin, Z. Liu, C. H. Yeh, K. Suenaga, and P. W. Chiu, ACS Nano **7**, 2587 (2013).

[23] Z. Sun, Z. Yan, J. Yao, E. Beitler, Y. Zhu, and J. M. Tour, Nature **468**, 549 (2010).

[24] A. W. Robertson and J. H. Warner, Nano Lett. **11**, 1182 ((2011).

[25] X. Zhang, L. Wang, J. Xin, B. I. Yakobson, and F. Ding, J. Am. Chem. Soc. **136**, 3040 (2014).